Nucleic Acids Research, 2024, 1–14
https://doi.org/10.1093/nar/gkad1218
Synthetic Biology and Bioengineering

Rapid human genomic DNA cloning into mouse artificial chromosome via direct chromosome transfer from human iPSC and CRISPR/Cas9-mediated translocation

Hitomaru Miyamoto[1], Hiroaki Kobayashi[2], Nanami Kishima[1], Kyotaro Yamazaki[3], Shusei Hamamichi[4], Narumi Uno[5], Satoshi Abe[4], Yosuke Hiramuki[4], Kanako Kazuki[4], Kazuma Tomizuka[5] and Yasuhiro Kazuki[1,2,3,4,*]

[1]Department of Chromosome Biomedical Engineering, Integrated Medical Sciences, Graduate School of Medical Sciences, Tottori University, 86 Nishi-cho, Yonago, Tottori 683-8503, Japan
[2]Department of Chromosome Biomedical Engineering, School of Life Science, Faculty of Medicine, Tottori University, 86 Nishi-cho, Yonago, Tottori 683-8503, Japan
[3]Chromosome Engineering Research Group, The Exploratory Research Center on Life and Living Systems (ExCELLS), National Institutes of Natural Sciences, 5-1 Higashiyama, Myodaiji, Okazaki, Aichi 444-8787, Japan
[4]Chromosome Engineering Research Center, Tottori University, 86 Nishi-cho, Yonago, Tottori 683-8503, Japan
[5]Laboratory of Bioengineering, Faculty of Life Sciences, Tokyo University of Pharmacy and Life Sciences, 1432-1 Horinouchi, Hachioji, Tokyo 192-0392, Japan

[*]To whom correspondence should be addressed. Tel: +81 859 38 6219; Fax: +81 859 38 6210; Email: kazuki@tottori-u.ac.jp

Abstract

A 'genomically' humanized animal stably maintains and functionally expresses the genes on human chromosome fragment (hCF; <24 Mb) loaded onto mouse artificial chromosome (MAC); however, cloning of hCF onto the MAC (hCF-MAC) requires a complex process that involves multiple steps of chromosome engineering through various cells via chromosome transfer and Cre-loxP chromosome translocation. Here, we aimed to develop a strategy to rapidly construct the hCF-MAC by employing three alternative techniques: (i) application of human induced pluripotent stem cells (hiPSCs) as chromosome donors for microcell-mediated chromosome transfer (MMCT), (ii) combination of paclitaxel (PTX) and reversine (Rev) as micronucleation inducers and (iii) CRISPR/Cas9 genome editing for site-specific translocations. We achieved a direct transfer of human chromosome 6 or 21 as a model from hiPSCs as alternative human chromosome donors into CHO cells containing MAC. MMCT was performed with less toxicity through induction of micronucleation by PTX and Rev. Furthermore, chromosome translocation was induced by simultaneous cleavage between human chromosome and MAC by using CRISPR/Cas9, resulting in the generation of hCF-MAC containing CHO clones without Cre-loxP recombination and drug selection. Our strategy facilitates rapid chromosome cloning and also contributes to the functional genomic analyses of human chromosomes.

Graphical abstract

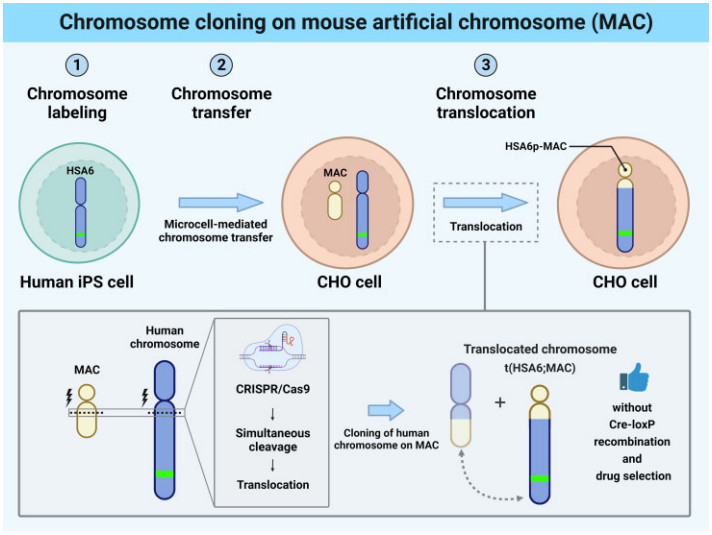

Received: August 29, 2023. **Revised:** November 26, 2023. **Editorial Decision:** December 9, 2023. **Accepted:** January 3, 2024

Introduction

A 'genomically' humanized animal is generated by transfer of cloned long-stranded human genomic DNA containing genes of interest, their *cis*-regulatory elements, and higher-order chromatin structure (1–3). In particular, this animal can be used to elucidate the role of chromatin domains through temporal analysis including developmental processes, and spatial analysis focusing on cellular and tissue expression patterns. To clone large human genomic DNA, bacterial artificial chromosomes (BACs) (4), P1 phage-derived artificial chromosomes (PACs) (5) and yeast artificial chromosomes (YACs) (6) have been used, and up to 900 kb genomic DNA has been successfully introduced into mice. In addition, further advancing the potential to incorporate additional genomic components, recently developed mouse artificial chromosomes (MACs) have achieved the delivery of up to 24 Mb human chromosome fragment (hCF) into mice with stable intra-individual retention and germline transmission, cumulating in generation of hCF containing animal models termed transchromosomic (TC) animals (3,7,8). These hCF-containing MACs (hCF-MACs) enabled TC animals to express human-like temporal and tissue-specific gene regulation, and are also useful for drug safety evaluation, disease mechanism studies, and pharmacological research (8,9).

Due to considerable complexity associated with multiple chromosome transfers and modifications, the construction of hCF-MACs remains challenging. As an initial step, due to limited proliferation capacity, chromosome-labeled human primary cell as donor is generally transformed via fusion with mouse A9 cell to initially generate human-A9 hybrid cell (Figure 1A, steps 1 and 2) (10,11). To isolate a single human chromosome, the chromosome is required to be transferred again from the hybrid to separate A9 cell through the process termed microcell-mediated chromosome transfer (MMCT) (Figure 1A, step 3) (10). MMCT is an attractive technology for cell-to-cell transfer of a microcell containing a single mammalian chromosome to a desired recipient cell (12,13). For instance, specific cell line [e.g. mouse A9, chicken DT40 or Chinese hamster ovary (CHO) cell as a donor cell] is cultured with mitotic inhibitor colcemid to form various micronuclei encapsulating a single or small number of chromosomes (14–16). These micronuclei are further separated by centrifugation and filtration as desired microcells used for MMCT. Further complicating the process, MMCT is performed again to transfer the isolated human chromosome into DT40 cell, a well-known cell line for high proficiency in homologous recombination (HR), wherein loxP site is inserted into target region by HR (Figure 1A, steps 4 and 5) (17,18). As the last step of this lengthy procedure, the hCF is subsequently transferred into MAC-harboring CHO cell in which the hCF with loxP is translocated onto the MAC with loxP by Cre expression to construct hCF-MAC (Figure 1A, steps 6 and 7) (8,9,19). Collectively, these steps involve multiple cloning and chromosome transfer, and require proficiency in the use of specialized equipment such as high-capacity centrifuges, strict control of cell proliferation, and adeptness in cell fusion methods, all of which are compounded by low efficiency.

Given the necessity for animal models that recapitulate human structural and functional dynamics at the genome level, yet the complexity associated with generating these models, we focused on three major points: (i) direct isolation of human chromosomes from human induced pluripotent stem cells (hiPSCs) (20) as chromosome donors and bypassing the use of human-A9 hybrids, (ii) efficient micronucleation by combined treatment with paclitaxel (PTX) and reversine (Rev), instead of colcemid and (iii) CRISPR/Cas9 genome editing system mediated chromosome translocation (21,22), and avoiding loxP integration in the DT40 cells and Cre-loxP recombination in the CHO cells. hiPSCs as chromosome donors possess infinite proliferation potential, but unlike cancer cells, these cells offer the intact genome with minimal occurrence of unexpected mutations, as well as the ease of chromosome labeling by genome editing and cloning (23,24). Compared with colcemid as a conventional micronucleation inducer, a combination of PTX and Rev resulted in improved micronucleation in the CHO cells (25). The microtubule destabilizer colcemid results in mitotic arrest and chromosome passive diffusion-dependent micronucleation whereas the microtubule stabilizer PTX can induce micronucleation in a mitotic arrest-independent manner (25–27). Rev inhibits mitotic checkpoints, which are part of the mechanism by which microtubule inhibitors induce cell death (28). Therefore, we attempted to further extend the applicability by testing their potential to induce direct micronucleation in hiPSCs. In addition, the recent reports indicated that CRISPR/Cas9 genome editing technology enabled site-specific modification of human chromosomes and MACs in the CHO cells (29). CRISPR/Cas9 has been documented to induce chromosomal translocations through simultaneous cleavage of multiple chromosomes (22,30), thereby suggesting its potential to induce site-specific cleavages and translocations in human chromosomes and MACs in the CHO cells.

Here, we aimed to develop a rapid and efficient method for hCF-MAC construction by evaluating these three alternative techniques using hiPSCs as chromosome donors in MMCT, PTX and Rev as inducers of micronucleation, and CRISPR/Cas9 genome editing for site-specific translocations. First, hiPSC were used for chromosome labeling with CRISPR/Cas9 and verification of PTX and Rev co-treatment induced micronucleation (Figure 1B, steps 1 and 2). Second, we attempted to transfer a model human chromosome 6 (HSA6) or 21 (HSA21) into MAC-containing CHO cell by MMCT using hiPSC donor (Figure 1B, step 2). Third, the hCF-MAC was constructed by translocation through simultaneous cleavage of MAC and human chromosome by genome editing, and cloning was performed (Figure 1B, step 3). Collectively, this simplified hCF cloning method shortens the acquisition and introduction of Mb-scaled human genomic DNA and accelerates human genome research by generating genomically humanized animals in the future.

Materials and methods

Cell culture

HFL1-iPS cells, derived from the reprogramming of human fetal lung fibroblasts HFL-1 (RCB0521), were established using a sendai virus vector system (ID pharma, Tsukuba, Japan) as described previously (31). After adapting to a feeder-free condition, HFL1-iPS cells were cultured on dishes coated with 0.5 μg/cm^2 iMatrix-511 silk (Nippi, Tokyo, Japan) in StemFit AK02N medium (Ajinomoto, Tokyo, Japan). During passaging of feeder-free cells, cells were cultured in the presence of 10 μM Y27632 (Fujifilm-Wako, Osaka, Japan) among 24 h after single-cell detachment. The establishment and maintenance HSA6-labeled HFL1-iPS (HFL1-L6) cells, with hygromycin B resistant gene (HygroR) insertion into HSA6, were performed in selection medium containing 50 μg/ml hygromycin B (Fujifilm-Wako). The establishment and main-

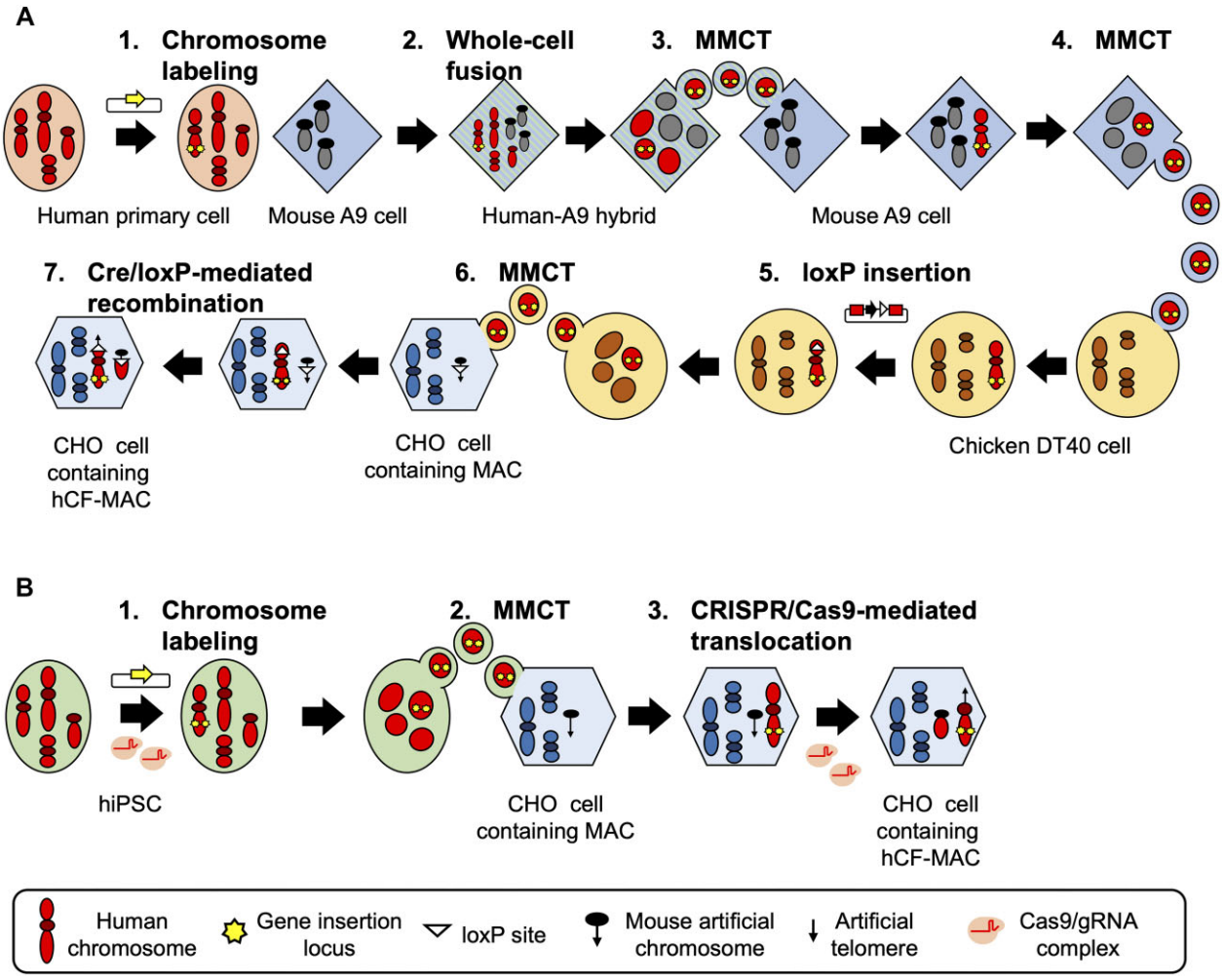

Figure 1. Comparative schematic diagram of the previous and optimized hCF-MAC construction. (**A**) Schematic diagram represents the previous method, simplified to show a minimum of seven steps, including chromosome labeling of human cell (step 1), whole-cell fusion of human cell and mouse A9 cell (step 2), MMCT into another A9 cell (step 3), MMCT into chicken DT40 cell (step 4), loxP insertion by homologous recombination in DT40 cells (step 5), chromosome transfer into CHO cell containing MAC (step 6), Cre-loxP recombination in CHO cell containing human chromosome and MAC (step 7). (**B**) Schematic diagram represents the optimized hCF-MAC construction method in this study, efficiently refined to include chromosome labeling of hiPSC (step 1), direct chromosome transfer from hiPSC into CHO cell containing MAC (step 2), CRISPR/Cas9-induced translocation between human chromosome and MAC in CHO cell (step 3). The diagrams visually highlight the considerable decrease in steps.

tenance of HSA21-labeled HFL1-iPS (HFL1-L21) cells, with neomycin resistant gene (NeoR) insertion into HSA21, were performed in selection medium containing 100 μg/ml G418 (Promega, Madison, WI, USA). CHO cell lines carrying MAC1 (32) or MAC2 (MI-MAC) (33) used were established previously. CHO cell lines with MAC1 were cultured in Ham's F-12 medium (Fujifilm-Wako) supplemented with 10% fetal bovine serum (FBS; Sigma Aldrich, St. Louis, MO, US), 1% penicillin-streptomycin solution (x100) (PS; Fujifilm-Wako), and 800 μg/ml G418. CHO cell lines with MAC2 were cultured in Ham's F-12 supplemented with 10% FBS, 1% PS and 300 μg/ml hygromycin B. CHO cell lines contain human chromosome and MAC, were cultured in Ham's F-12 supplemented with 10% FBS, 1% PS, 200 μg/ml hygromycin B and 800 μg/ml G418.

CRISPR/Cas9 genome editing

All genome editing reagents were purchased from the Alt-R® CRISPR-Cas9 System by Integrated DNA technologies (IDT; Coralville, IA, USA), and the associated protocols were followed. The crRNAs used for chromosome labeling were designed by inputting the target genomic background of target regions and PAM into CRISPOR (http://crispor.tefor.net) and selected. The crRNAs used for translocation were designed based on the genome of the species from which the target sequence was originated (i.e. human or mouse). Its compatibility with C_griseus_v1.0/criGri1 (Jul,2013) was verified using the gggenome browser (https://gggenome.dbcls.jp/en/), ensuring the absence of fewer than three base mismatches. The gRNA was prepared by adding annealing solution containing 200 pmol each of Alt-R®CRISPR-Cas9 crRNA and Alt-R®CRISPR-Cas9 tracrRNA at 95°C for 5 min. The gRNA was then mixed with 100 pmol Alt-R® S.p.Cas9 Nuclease V3 and incubated for over 20 min for ribonucleoprotein (RNP) formation. Following this, the mixture was introduced into an electroporation mixture containing 1×10^6 cells, which was then used for electroporation. See below for all crRNA target sequences and their uses (Supplementary Table S1).

Electroporation

Transfection of RNP and plasmid vector into HFL1-iPS cells, as well as introduction of RNP into CHO cells were performed using the NEPA21 Super Electroporator (NEPA GENE, Chiba, Japan). After each cell type was dissociated, it was washed with Opti-MEM® (ThermoFisher Scientific, Waltham, MA, USA). Subsequently, 1×10^6 cells were resuspended in a total of 100 μL electroporation mixture of Opti-MEM® with added RNP complex and 500 pmol single strand carrier DNA or 10 μg plasmid. HFL1-iPS cells received a perforating pulse of 125 V with a pulse width of 5.0 ms, while CHO cells received a perforating pulse of 150 V with a pulse width of 5.0 ms.

Plasmid construction

For labeling HSA6, the vector containing 500 bp homology arms (Left arm; chr6:120279418–120279917, Right arm; chr6:120279926–120280425, GRCh38/hg38) the gRNA cleavage sequence, and multiple cloning site (pUCIDT-Amp chr6T3) was synthesized (IDT DNA). HS4-CAG-mCherry-HS4-PGK-HygroR cassette was produced by replacing EGFP in the Bxb1neo-EGFP (34) plasmid with mCherry, and PGK-NeoR was replaced with PGK-HygroR derived from pMAC2 (32), and inserted into homology arm vector (pUCIDT-Amp chr6T3-HS4-CAG-mCherry-HS4-PGK-HygroR). For HSA21 labeling, pcDNA3.1-HS4-CAG-EGFP-HS4-PGK-NeoR was constructed by digestion with MluI-NotI and blunting NotI end of Bxb1neo-EGFP plasmid, as well as ligated with pcDNA3.1 backbone, which was digested with BstZ17I-MluI and excised from pcDNA3.1(+) (Thermo Fisher Scientific).

Chromosome labeling

For HSA6 labeling, pUCIDT-Amp chr6T3-HS4-CAG-mCherry-HS4-PGK-HygroR plasmid and gRNA-chr6T3 (chr6: 120279921–120279940, GRCh38/hg38) containing RNP, which cleaves HSA6 and plasmid simultaneously, were co-transfected into HFL1-iPS cells. For HSA21 labeling, pcDNA3.1-HS4-CAG-EGFP-HS4-PGK-NeoR, gRNA-21qteloT9 (chr21: 46670306–46670325, GRCh38/hg38) containing RNP, which cleaves HSA21, and gRNA-VIKING (35) containing RNP, which cleaves pcDNA3.1 backbone, were co-transfected into HFL1-iPS cells. After electroporation, transfected HFL1-iPS cells were seeded in five 10 cm dishes and selected by 50 μg/ml hygromycin B for HSA6 labeling or 100 μg/ml G418 for HSA21 labeling for 10 days. Colonies expressing fluorescent protein were then isolated and cultured separately to establish clones.

Cell confluency assay and micronuclei staining

HFL1-iPS cells were seeded at a density of 3×10^4 cells/well in 24-well plates. After 48 h, micronucleus induction StemFit AK02N medium was added. Cell confluence was monitored using an IncuCyte®S3 imaging system (SARTORIUS, Göttingen, Germany) at 0, 6, 12, 18, 24, 30, 36, 42 and 48 h after drug treatment. Each well was imaged at four distinct fields of view using a 10x objective lens. After initial 24 h post-induction, the medium was replaced with fresh micronucleus induction medium. The micronucleus induction StemFit AK02N medium added to the wells set for each condition contained one of the following treatments: colcemid (demecolcine; Sigma Aldrich) at a concentration of 0.1 μg/ml, paclitaxel (PTX; Fujifilm-Wako) at 20 nM, PTX at 100 nM, or a combination of PTX at 100 nM and reversine (Rev; Cayman Chemical, Ann Arbor, MI, USA) at 1000 nM. Three wells per treatment were evaluated as independent biological replicates and performed three times. The percent confluence was calculated for each field of view and the average of the four fields was used to represent each well at each time point. The mean confluence of three wells was then plotted over time for treatment conditions. Statistical analysis was performed using two-way ANOVA in GraphPad Prism8 (MDF, Tokyo, Japan) and $P < 0.001$ was considered statistically significant. This analysis compared the effects of treatment conditions, time, and their interaction on cell confluence. Microscopic images of micronuclei were captured using HFL1-iPS cells treated with PTX and Rev for 48 h. After detachment, the cells were treated with 0.075M KCl for 15 min, followed by fixation in methanol: acetic acid (3:1 in volume), and mounted on glass slides. The slides were then stained with the McIlvaine buffer, pH 4.5, containing quinacrine mustard. Imaging of the slide specimens was conducted using an Axio Imager Z2 (Carl Zeiss, BW, Germany) microscope with a 63× oil immersion objective lens.

Microcell-mediated chromosome transfer

Chromosome-labeled HFL1-iPS cells were seeded at 2×10^6 cells/flask in T25 flasks coated overnight with iMatrix-511 silk. Twenty-four hours post-seeding, the medium was replaced with micronucleus induction StemFit AK02N medium containing 100 nM PTX, 1000 nM Rev and 5% KnockOut® Serum Replacement (Thermo Fisher Scientific; Gibco), and changed again after another 24 h. Following micronucleus induction, cells were enucleated in the D-MEM (Fujifilm-Wako) with 10 μg/ml cytochalasin B (Sigma Aldrich) and centrifugation at 8000 RPM for 1 h by JLA-10.500 rotor of Avanti J series (Beckman Coulter, Pasadena, CA, USA) (25). Microcell pellets were collected and subjected to purification through filtration using 8, 5, and 3 μm pore size of membrane filters (Cytiva; Whatman, Tokyo, Japan). The purified microcells were bridged to CHO cells with phytohemagglutinin PHA-P (Sigma Aldrich) and fused with a polyethylene glycol 1000 (Fujifilm-Wako) D-MEM solution. Microcells from six flasks were fused with 2×10^6 cells in a 6 cm dish, which had been seeded the day before. The post-fusion cells were seeded and subjected to selection culture starting at 24 h later.

Fluorescent *in-situ* hybridization analysis

Cells were treated with metaphase arresting solution (Genial Helix, Chester, UK) at 1.0 μg/ml for 1 h, followed by treatment with 0.075 M KCl for 15 min, and fixed in methanol: acetic acid (3:1 in volume). The fixed cells were spread onto slides. Slide specimens underwent denaturation in 70% formamide 2× SSC solution at 70°C, followed by dehydration in cold ethanol. Probe DNA for each target was generated using template DNA and dNTPs, along with digoxigenin-11-dUTP or biotin-16-dUTP, utilizing the Nick Translation Mix (Roche, Basel, Swiss), denatured, and rapidly cooled before hybridizing overnight on slides. Hybridized slides were washed with 50% formamide 2× SSC buffer, and fluorescently labeled with 4xSSC/1% BSA solution containing anti-digoxigenin-rhodamine, Fab fragments (Roche), and streptavidin Alexa Fluor® 488 conjugate (Life Technologies, Carlsbad, CA, USA). Fluorescently

labeled slides were washed with 4xSSC buffer containing Triton X-100 (Sigma Aldrich) and sealed with a mounting medium containing DAPI. Metaphase images were captured using Axio Imager Z2 and Metafer (Meta Systems, BW, Germany) and analyzed with Isis software (Carl Zeiss). Probe DNA was used in the following target DNA:probe name combinations, *HLA-A* (HSA6):CH501-309N1 (BACPAC Resources Center, Emeryville, USA), D21Z1(HSA21):p11-4, human DNA (whole human chromosome):human Cot-1 DNA (Thermo Fisher Scientific; invitrogen), mouse DNA (whole mouse chromosome):mouse Cot-1 DNA (invitrogen), FOXF2 (HSA6):RP11-13F18 (Advanced GenoTechs Co., Tsukuba, Ibaraki, Japan), ATXN1 (HSA6):RP11-91N3 (Advanced GenoTechs Co.). All BAC probes were digested by EcoRI-HF and BamHI-HF (New England BioLabs, Ipswich, Massachusetts, USA) and purified before biotinization or digoxigenination. The mBAND-FISH analysis employed the XCyte 21 human mBAND probe (MetaSystems), in accordance with standard protocols of the manufacturer.

Surveyor nuclease assay

Cells transfected with RNP underwent a recovery culture for 48 h. Subsequently genomic DNA was extracted using Puregene Kits (QIAGEN, Limburg, Netherlands). PCR amplification was performed using primers flanking the target sequences (Figures S2, S3 and Table S2) and TaKaRa ExTaq® (Takara Bio, Shiga, Japan). The amplicons were subjected to a thermal cycling process at 95°C for 10 min, ramping down from 95°C to 85°C at a rate of −2°C/s, followed by 85°C to 25°C at −0.1°C /s, then holding at 25°C for 1 min and finally at 4°C. Double-stranded DNA with mismatches resulting from genome editing-induced insertions and deletions were cleaved by Surveyor Nuclease S (IDT). Agarose gel electrophoresis was used to separate the cleaved products, and ImageJ (36) was utilized for analysis. The proportion of cleaved DNA was calculated based on the band intensities.

CRISPR/Cas9-mediated chromosome translocation and sequential enrichment cloning

CHO cells harboring both human chromosomes and MAC were transfected with two types of pre-validated RNP. Post-transfected, cells were seeded into two dishes. After a 48-hr recovery period, genomic DNA was extracted from the cells in one dish and used for Junction DNA detection. Cells from the other dish were seeded into a 96-well plate at densities of 10 or 100 cells/well. Upon reaching approximately 90% confluence, cells were detached by 0.1% trypsin/0.04% EDTA, with 90% of the cells sampled for PCR and the remaining 10% cultured further with fresh medium. The sampled cells were washed with PBS, resuspended in sterile water, and subjected to a pre-treatment at 95°C for 10 min. Genomic PCRs with the crude samples were conducted by adding the pre-treated cells to a PCR plate dispensed with KOD One® PCR Master Mix -Blue- (Toyobo, Osaka, Japan) adjusted with appropriate primers (Table S2). Wells in which junction DNA amplification was confirmed were further diluted. When junction DNA amplification was observed at 10 cells/well, a limiting dilution was performed at 1 cell/well to detect single colony. Wells with single colonies were clonally expanded and screened for the presence of junction DNA by PCR. Sanger sequencing was performed using the junction PCR amplification product derived from the bulk genome of 10 cells/well as a template. The sequencing analysis was carried out on an Applied Biosystems 3730xl DNA Analyzer (Thermo Fisher Scientific) with the DNA sequencing analysis service provided by Fasmac Co., Ltd.

Results

Donorization of chromosome-labeled hiPSCs

In this study, drug resistant genes were integrated into the target chromosomes of HFL1-iPS cells to isolate chromosome-transferred clones by MMCT. The HFL-1 cells were traditionally used as a resource of human chromosome for human-A9 hybrid cells (2), and we established HFL1-iPS cells by Sendai-virus as described previously (31). We selected two human chromosomes of different size and function as model chromosomes; HSA6, which contains the immunologically important human leukocyte antigen (HLA) gene cluster, and HSA21, which is the cause of the Down syndrome phenotype and the largest hCF ever introduced into mouse via MAC. For HSA6, a specific labeling vector with marker gene cassette flanked by 500 bp homology arms and gRNA recognition sequence was constructed to target a non-genic region in HSA6q22.3 (Figure 2A). After hygromycin B selection of RNP and vector co-transfected cells, isolated HFL1-L6 clones showed resistance to hygromycin B and expression of mCherry fluorescence (Figure 2B). These clones were confirmed to have a drug resistant gene inserted on HSA6 by fluorescent *in situ* hybridization (FISH) analysis using a BAC containing to *HLA-A* region on HSA6 and the targeting vector as a probe (Figure 2C). In the case of HSA21, we used the versatile NHEJ-based knock-in for genome editing (VIKING) by using RNP to insert a non-specific vector (Figure 2D). Insertion of marker genes in the HFL1-L21 clones with G418 resistance and EGFP fluorescence were further confirmed by FISH using D21Z1 α-satellite and the non-specific vector DNA as probes (Figure 2E, F).

Chromosome transfer from HFL1-iPS clones to CHO cells containing MAC

Before chromosome transfer, we verified condition of micronucleus induction for HFL1-iPS cells. Treatment with colcemid, a microtubule destabilizer, has been used for conventional micronucleus induction for cells and treatment with PTX and Rev has been newly reported as alternative micronucleus-inducing method (25). Therefore, we performed a brief comparison of these two micronucleation methods in hiPSCs. After micronucleus induction, the cell confluence of HFL1-iPS cells at 48 hrs was profoundly suppressed by 0.1 μg/ml colcemid as well as 20 and 100 nM PTX, but was rescued by the co-treatment of PTX and Rev (Figure S1a, b). The HFL1-iPS cells treated with both PTX and Rev showed micronucleus formation (Figure S1c). Given these findings, we performed MMCT taking advantage of the micronucleus formation facilitated by co-treatment with PTX and Rev.

MMCT from the labeled HFL1-iPS cell clones to CHO cells harboring MAC was performed. Microcells harvested by centrifugation after culturing in micronucleation media supplemented with PTX and Rev, were fused with the recipient CHO cells (Figure S2a, b). In all MMCT experiments with independent HFL1-iPS donor cells, colonies with drug resistance and fluorescence were obtained, indicating successful transfer of the labeled human chromosomes (Table 1). One or two colonies obtained from each transfer of HSA6 into CHO

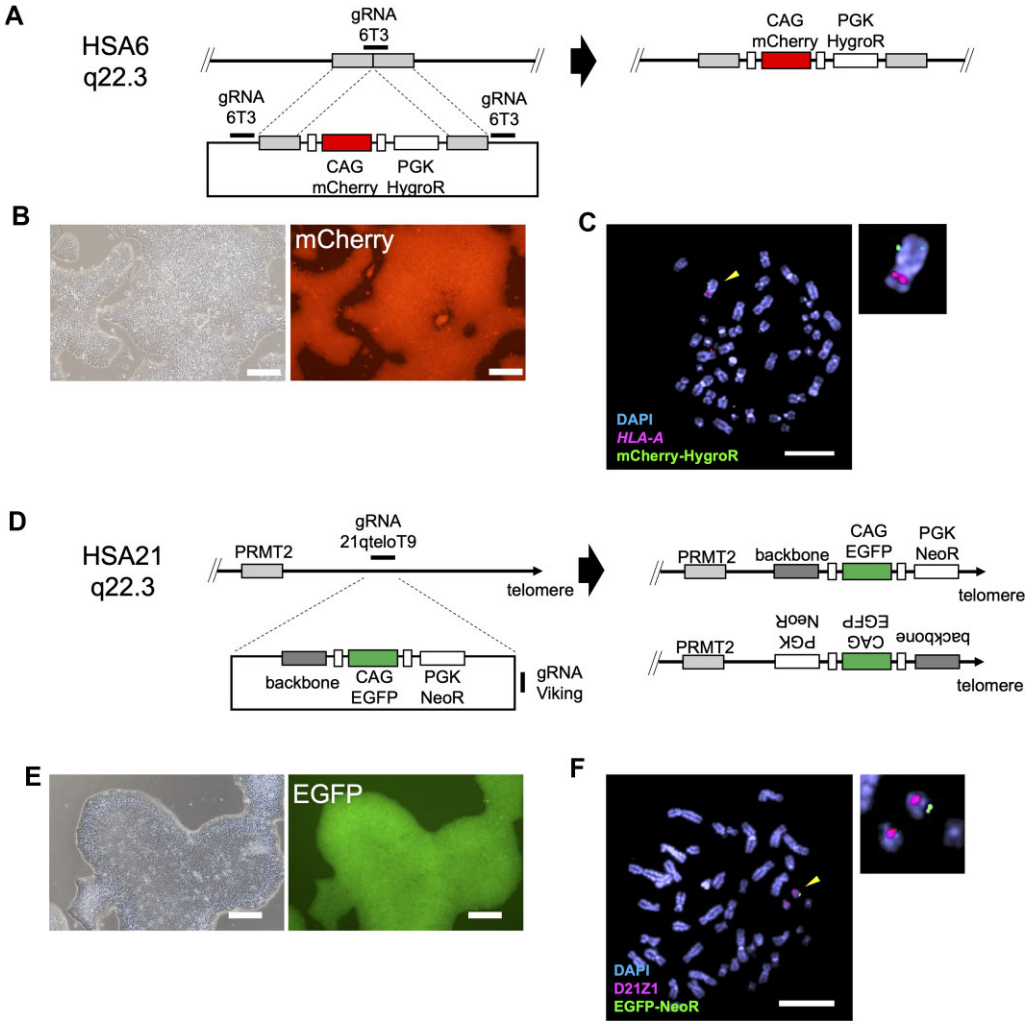

Figure 2. Chromosome labeling of hiPSC. (**A**) Scheme for insertion of selection marker (HS4-CAG-mCherry-HS4-PGK-HygroR) by co-transfection of the specific targeting vector and single RNP induced homology-dependent recombination on HSA6. The specific targeting vector also contains homologous arms flanked by gRNA-6T3 recognition sequence, and when introduced into the cell, cleavage occurs simultaneously with the same sequence on HSA6. (**B**) Representative brightfield and fluorescent images of hygromycin resistant HFL1-L6 clone. Scale bars represent 200 μm. (**C**) FISH on metaphase spreads of HFL1-L6 clone with *HLA-A* specific BAC probe (CH501-309N1, red signal) and targeting vector (green signal). Yellow arrowhead denotes the labelled HSA6 with a magnified view. Scale bars represent 10 μm. (**D**) Scheme for insertion of selection marker (HS4-CAG-EGFP-HS4-PGK-NeoR) by co-transfection of targeting vector and two Cas9-RNPs induced non-homologous end joining on HSA21. Targeting vector with pUC backbone and HSA21 are simultaneously cleaved by gRNA-VIKING and gRNA-21qteloT9, respectively. (**E**) Representative brightfield and fluorescent images of G418 resistant HFL1-L21 clone. Scale bars represent 200 μm. (**F**) FISH on metaphase spreads of HFL1-L21 clone with HSA21 α-satellite specific probe (p11-4, red signal) and targeting vector (green signal). Yellow arrowhead denotes the labeled and non-labeled HSA21 with a magnified view. Scale bars represent 10 μm.

MAC1 cells showed EGFP fluorescence derived from MAC1 and mCherry fluorescence derived from HSA6 (Figure 3A, Table 1). These colonies were subsequently cloned as CHO MAC1/HSA6 and confirmed that the presence of single submetacentric human chromosome and MAC was detected in half of the clones by FISH analysis (Figure 3B, Table 2). Additional mapping FISH of the *HLA-A* and marker genes revealed that the transferred human chromosome originated from the labeled HSA6 (Figure 3C). The same approaches were used to transfer HSA21 to CHO MAC2 cells, resulting in over seven colonies obtained from each transfer (Figure 3D, Table 2). The retention of single acrocentric human chromosome and MAC was confirmed centromere DNA and marker gene mapping confirming derivation from labeled HSA21 (Figure 3E,F). The clones with combined retention of each human chromosome and MAC with more than 70% metaphase were obtained (Table S3). This result indicates the capacity of transferring a single chromosome from hiPSCs to CHO cells directly without production of human-A9 hybrid cells.

Simultaneous cleavage and translocation for human chromosome and MAC by CRISPR/Cas9

CRISPR/Cas9 gRNAs were designed for each chromosome to induce double strand break and translocation of human chromosomes and MACs (Table S1). The mouse chromosome 11 (MMU11) derived sequence on the MACs was used as a target of MAC cleavage (Figure S3a, c). The designated cleavage site for HSA6 was *COL11A2* (Figure S4a), while for HSA21 it was a pseudogene *ANKRD30BP2* (Figure S4c). These sites were located on the centromeric side of the HLA gene cluster or HSA21 long arm and were suitable as translocation sites. Following the introduction of RNP into CHO MAC1, CHO MAC2, HFL1-iPS, and CHO MAC2/HSA21 cells, a surveyor

Table 1. Number of drug resistant colonies derived from hiPSC donors and associated MMCT efficiencies

Donor clone	Recipient	No. of colony		Avg. of MMCT efficiency (no. of colony/no. of recipient cell)
		Exp.1	Exp.2	
HFL1-L6#07	CHO MAC1	1	2	7.5×10^{-7}
HFL1-L6#10	CHO MAC1	3	1	1.0×10^{-6}
HFL1-L6#16	CHO MAC1	2	1	7.5×10^{-6}
HFL1-L21#06	CHO MAC2	32	NT	1.6×10^{-5}
HFL1-L21#10	CHO MAC2	7	NT	3.5×10^{-6}
HFL1-L21#16	CHO MAC2	18	NT	9.0×10^{-6}

NT: Not tested.

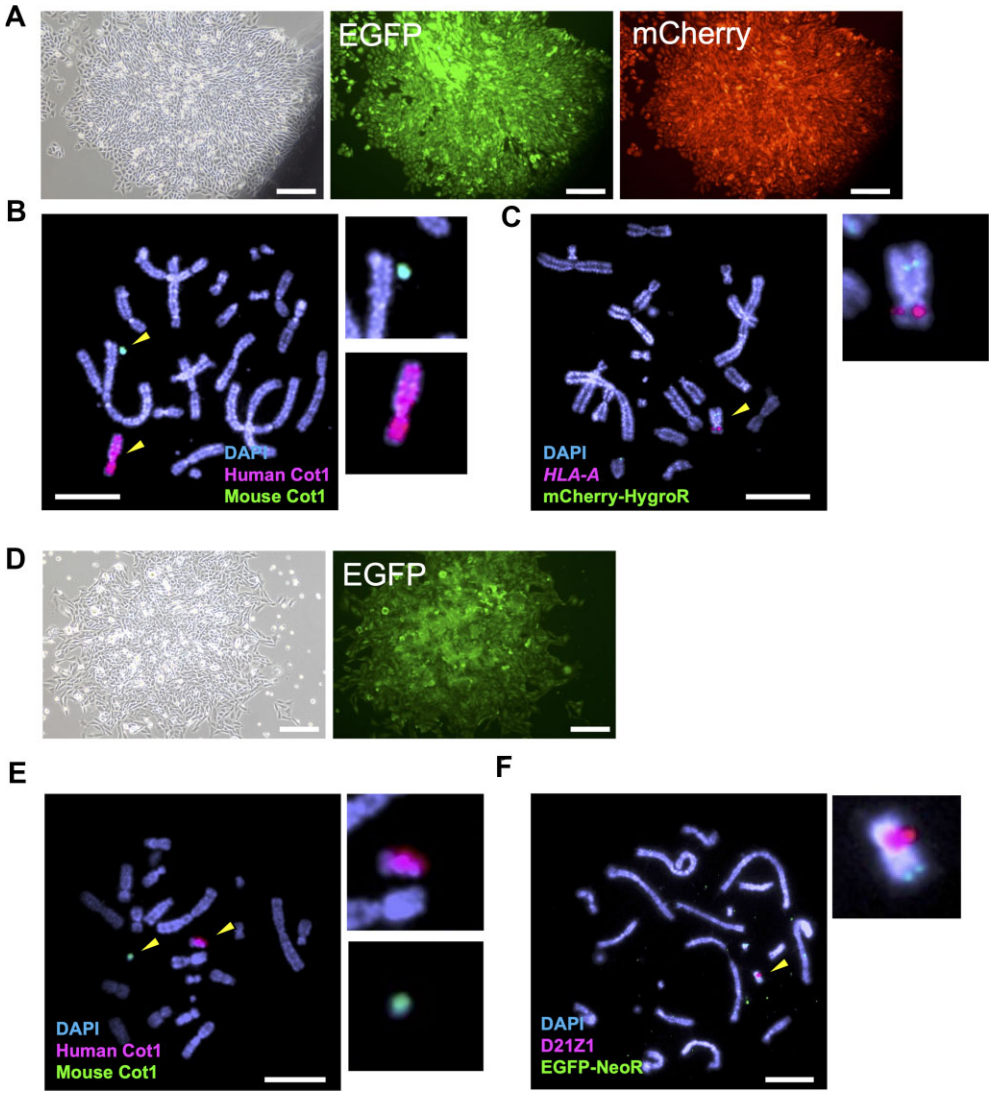

Figure 3. Direct chromosome transfer from hiPSCs to CHO-MAC cells. (**A**, **D**) Representative brightfield and fluorescent images of the hygromycin and G418 co-resistant CHO colony. Scale bars represent 200 μm. (**B**, **C**) FISH on metaphase spreads of CHO MAC1/HSA6 #07-2 clone with human DNA specific probe (human Cot-1, red signal) and mouse DNA probe (mouse Cot-1, green signal), or *HLA-A* specific probe (CH501-309N1, red signal) and targeting vector (green signal). Yellow arrow heads denote the MAC1 and HSA6 with a magnified view. Scale bars represent 10 μm. (**E**, **F**) FISH on metaphase spreads of CHO MAC2/HSA21 #06-1 clone with human DNA specific probe (human Cot-1, red signal) and mouse DNA probe (mouse Cot-1, green signal), or HSA21 α-satellite specific probe (p11-4, red signal) and targeting vector (green signal). Yellow arrowheads denote the MAC2 and HSA21 with a magnified view. Scale bars represent 10 μm.

Table 2. FISH analysis of MAC/HSA clones

Clone name	Frequency of metaphase with single MAC and hChr (%)	Most frequent karyotype	
CHO MAC1/HSA6 #07–2	86.7	2n, +MAC, +hChr	[26/30]
CHO MAC1/HSA6 #07–3	90.0	2n, +MAC, +hChr	[27/30]
CHO MAC1/HSA6 #10–2	70.0	2n, +MAC, +hChr	[21/30]
CHO MAC1/HSA6 #10–3	26.9	2n, +MAC, +hChrx2	[9/26]
CHO MAC1/HSA6 #16–2	10.0	2n, +MAC, +hChrx2	[17/20]
CHO MAC1/HSA6 #16–3	0.0	2n, +MAC	[6/10]
CHOMAC2/HSA21 #06–1	100.0	2n, +MAC, +hChr	[10/10]
CHOMAC2/HSA21 #06–2	70.0	2n, +MAC, +hChr	[14/20]
CHOMAC2/HSA21 #10–2	75.0	2n, +MAC, +hChr	[15/20]
CHOMAC2/HSA21 #10–4	0.0	2n, +MAC, +hChr(der)	[4/4]
CHOMAC2/HSA21 #16–2	20.0	2n, +MAC, +hChr, +hChr(frag)x1∼6	[5/10]
CHOMAC2/HSA21 #16–3	22.2	2n, +MAC, +hChr, +hChr(frag)	[6/9]

2n: diploid, 4n: tetraploid, +hChr: additional target human chromosome, +MAC; additional mouse artificial chromosome, +hChr(der): unknown origin derivative human chromosome, +hChr(frag): unknown origin human chromosome fragment.

nuclease assay was used to assess genomic DNA at 72 h after genome editing (Tables S1, S2). The gRNAs that showed cleavage activity (percentage of indels; MAC1 T2-1: 15.2%, MAC2 T2-3 21.5%, COL11A2 T1-1: 21.3%, 21qCen T2-1: 16.2%) were used for subsequent experiments (Figures S3b, d and S4b, d). It should be noted that 21qCen T2-1 has multiple off-targets within the human genome, although it selectively cleaves HSA21 in the Chinese hamster genome background.

Next, we evaluated the capacity of the simultaneous cleavage using CRISPR/Cas9 against human chromosomes and MACs in CHO cells to induce chromosomal translocations. First, construction of the HSA6p-MAC was performed by translocation of HSA6 to MAC (Figure 4A). After electroporation of RNP into CHO MAC1/HSA6, the presence of translocated DNA was confirmed by bulk genomic PCR analysis (Figure S5a). The translocated DNA that appeared in this process was predicted to be derived from the HSA6p-MAC junction (<700 bp) and the by-product junction (<450 bp) that resulted from joining the residual sequences together, and we tried to detect both patterns using the primer used in the surveyor nuclease assay (Table S2). Two types of translocated DNA were amplified only under the condition of simultaneous cleavage of HSA6 and MAC and the detection limit was 10 ng (≒1500 cells) of genomic DNA (Figure 4B). Since cloning by limiting dilution was considered difficult, we developed a method of stepwise enrichment cloning (Figure S5a). In this method, a fixed number of cell pools were seeded onto 96-well plates, and after recovery culture, sampling and PCR were performed to identify pools including the cells harboring the translocated DNA, which were further diluted and seeded repeatedly. This was repeated to increase the enrichment of the cells harboring translocated DNA in the pool and finally the cells were cloned. A HSA6p and MAC translocated DNA-positive pool was successfully obtained from 10 cells/well (Figure 4C), followed by a translocated DNA-positive single colony from 1 cell/well (Figure 4D). The amplified translocated DNA sequence derived from 10 cells/well was identified by Sanger sequence reads as chimeric DNA between MMU11 on MAC1 and *COL11A2* on HSA6 (Figure 4E). This sequence was caused by a micro rearrangement involving the joining of 3 bp upstream of the PAM in MAC1 T2-1 and 28 bp upstream of the telomere side of COL11A2 T1-1, and the deletion of 2 bp upstream of the PAM (Figure S6a). FISH analysis of the established clones revealed the detection of hCF-translocated MAC; t(MAC;hChr) and the p-arm deleted HSA6 (Figure 4F). The translocation-positive clones, established as CHO HSA6p-MAC1, were retained at a frequency of average 90 (±12.6, S.D.)% and stably retained the target chromosome (Table 3, Table S4). FISH analysis confirmed that the HSA6 and HSA6p-MAC1 in the CHO cells contained 6p21.3 (*HLA-A*), 6p22.3 (*ATXN1*) and 6p25.3 (*FOXF2*), as well as the original HSA6 in the HFL1-L6 cell (Figure S7).

We further validated the same translocation induction and sequential enrichment cloning method in CHO MAC2/HSA21 (Figure 5A, Figure S5). The expected translocated DNA derived from the HSA21q-MAC2 junction (<400 bp) and by-product junction (<1500 bp) was amplified from 100 ng of the bulk genome of CHO MAC2/HSA21, in which we induced simultaneous breakage of MAC2 and HSA21 (Figure 5B). Therefore, to detect translocated cells with higher sensitivity, we seeded post-genome-edited cells at 100 cells/well and 2 wells of translocated DNA-positive cells were obtained (Figure 5C). Sanger sequencing analysis confirmed the specific amplicons derived from 10 cells/well, which was enriched from two 100 cells/well pools. These amplicons were constructed by MMU11 on MAC2 and *ANKRD30BP2* on HSA21 translocated DNA, differing by 2 bp near the junction (Figure 5D, Figure S6b). After cloning, FISH analysis was performed and CHO HSA21q-MAC clones were identified that harbored MAC with hCF translocated and HSA21 with the long arm deleted (Figure 5E, Table 3, Table S4). mBAND analysis confirmed that the translocated fragment of HSA21q remained the original band pattern, and we did not observe any significant structural alterations in the HSA21q (Figure S8). Thus, using multiple human chromosomes as models, our findings indicated that simultaneous cleavages of MAC and human chromosomes in CHO cells can induce site-specific translocation and construction of hCF-MAC.

Discussion

The conventional hCF-MAC construction requires a chromosome labeling step and at least four chromosome transfer steps including the generation of human-A9 whole-cell hybrids, the establishment of single human chromosome-retaining A9 cells, its introduction into the DT40 cells and CHO cells, and three additional modification processes, including chromosomal labeling, loxP insertion, and Cre-loxP recombination, for a total of seven steps (Figure 1A). In contrast, the

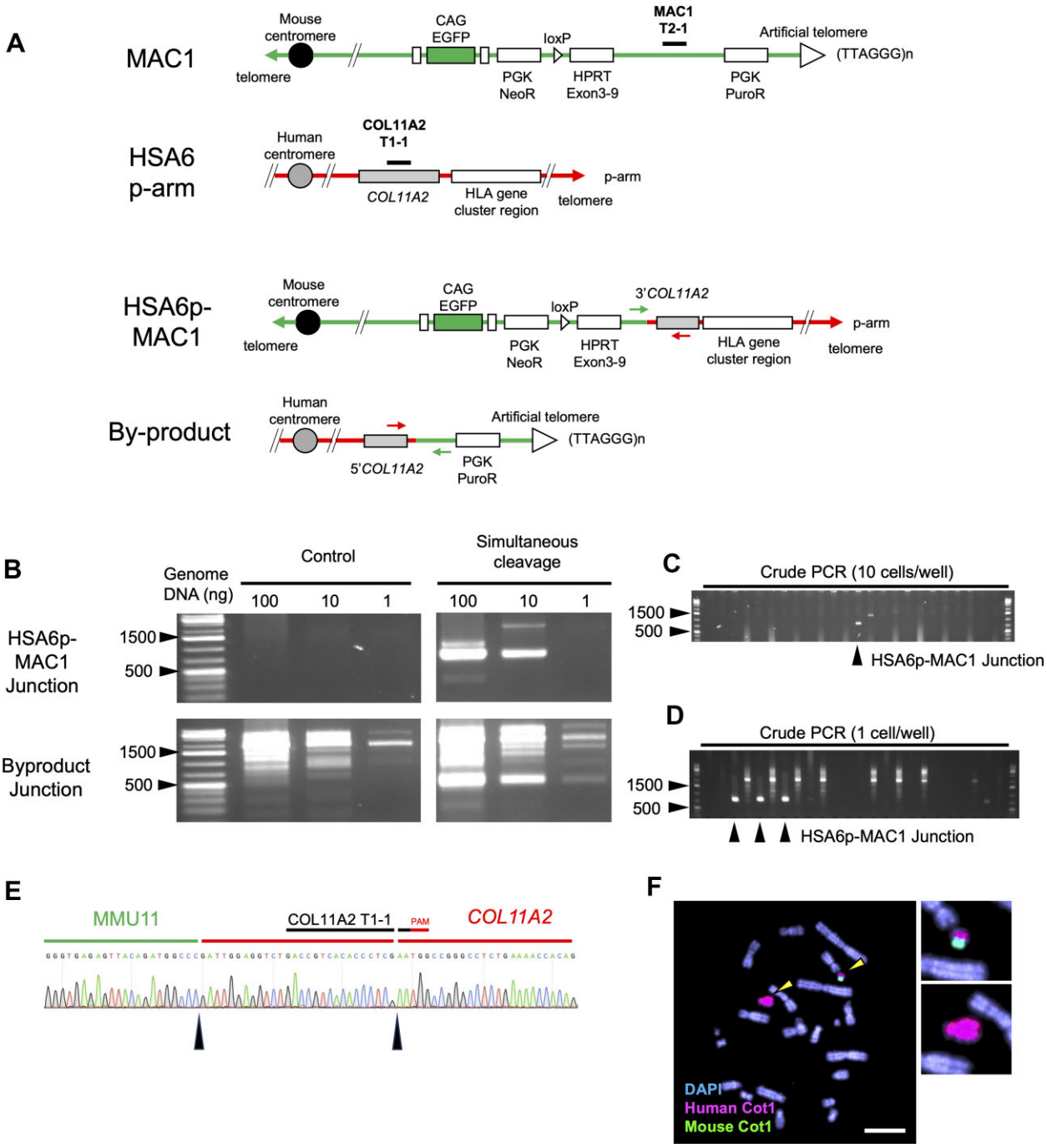

Figure 4. HSA6p-MAC1 construction via CRISPR/Cas9-mediated chromosome translocation. (**A**) Schematic representation of MAC1 and HSA6 with translocational regions highlighted. The subsequent panels depict the resulting HSA6p-MAC1 and by-product post-translocation. Red lines indicate human chromosome and green lines indicate mouse chromosome. Arrows indicate primer for detection of translocated DNA, and colors correspond to recognition chromosomes. (**B**) Agarose gel electrophoresis images of PCR-amplified products from bulk genomic DNA of CHO MAC1/HSA6 post-simultaneous cleavage induction of MAC1 and HSA6, or non-RNP introduced (Control). The top row shows the detection of translocated DNA (<700 bp) in HSA6p-MAC1 and the bottom row shows the by-product DNA (<450 bp). (**C**) Agarose gel electrophoresis image of crude PCR products derived from samples seeded at 10 cells/well. PCR product from each well is represented in two lanes: the left lane targets the by-product, while the right lane targets HSA6p-MAC1. (**D**) Agarose gel electrophoresis image of crude PCR products derived from 1 cell/well colonies. PCR product from each well is represented in two lanes: the left lane targets the HSA6p-MAC1, while the right lane targets by-product. (**E**) Sanger sequencing electropherogram excerpt, highlighting the translocation junction of genomic DNA samples derived from a pool of 10 cells. Black arrowheads show the breakpoints. (**F**) FISH on metaphase spreads of CHO HSA6p-MAC1 clone with human DNA specific probe (human Cot-1, red signal) and mouse DNA probe (mouse Cot-1, green signal). Yellow arrowheads denote the HSA6p-MAC1 and HSA6 with p-arm deletion with a magnified view. Scale bars represent 10 μm.

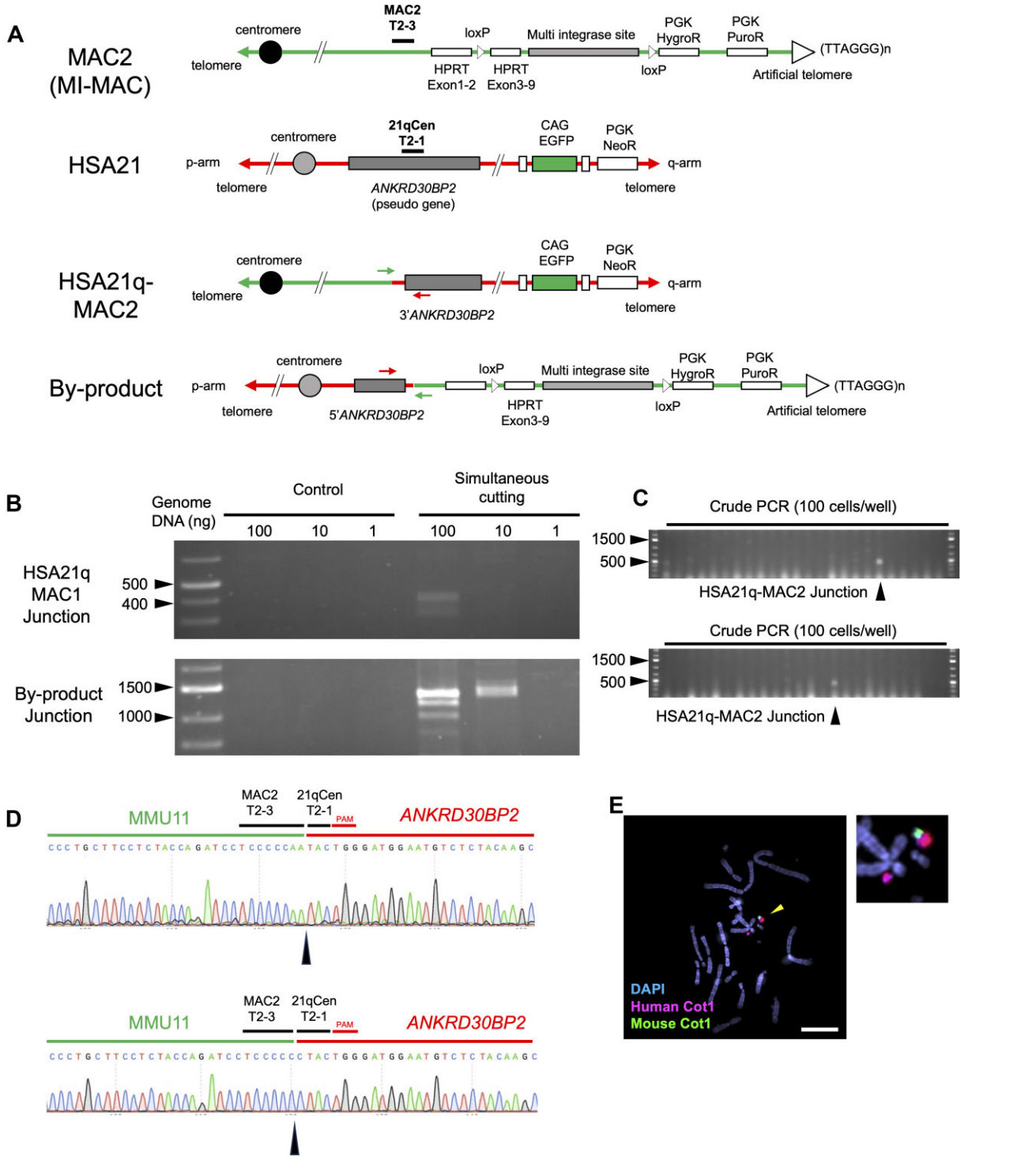

Figure 5. HSA21q-MAC2 construction via CRISPR/Cas9-mediated chromosome translocation. (**A**) Schematic representation of MAC2 and HSA21 with translocational regions highlighted. The subsequent panels depict the resulting HSA21q-MAC2 and by-product post-translocation. Red lines indicate human chromosome and green lines indicate mouse chromosome. Arrows indicate primer for detection of translocated DNA, and colors correspond to recognition chromosomes. MAC2-derived MI-MAC was used in this study. (**B**) Agarose gel electrophoresis images of PCR-amplified products from bulk genomic DNA of CHO MAC2/HSA21q post-simultaneous cleavage induction of MAC2 and HSA21 or non-RNP introduced (Control). The top row shows the detection of translocated DNA (<400 bp) in HSA21q-MAC2 and the bottom row shows the by-product DNA (<1500 bp). (**C**) Agarose gel electrophoresis image of crude PCR products derived from samples seeded at 100 cells/well. PCR product from each well is represented in two lanes: the left lane targets the by-product, while the right lane targets. (**D**) Sanger sequencing electropherogram excerpt highlighting the translocation junction of two independent 100-cell pools genomic DNA samples after enrichment by 10-cell pools. Black arrowheads show the breakpoints. (**E**) FISH on metaphase spreads of CHO HSA21q-MAC2 clone with human DNA specific probe (human Cot-1, red signal) and mouse DNA probe (mouse Cot-1, green signal). Yellow arrow heads denote the HSA21q-MAC2 and HSA21 with q-arm deletion with a magnified view. Scale bars represent 10 μm.

Table 3. FISH analysis of hCF-MAC clones

Clone name	Frequency of metaphase with MAC-hChr translocation (%)	Most frequent karyotype	
CHO HSA6p-MAC1 #01	65.0	2n, +t(MAC;hChr), +hChr(del)	[10/20]
CHO HSA6p-MAC1 #02	100.0	2n, +t(MAC;hChr), +hChr(del)	[16/20]
CHO HSA6p-MAC1 #03	100.0	2n, +t(MAC;hChr), +hChr(del)	[24/30]
CHO HSA6p-MAC1 #04	100.0	2n, +t(MAC;hChr)x2, +hChr(del)	[20/24]
CHO HSA6p-MAC1 #05	85.0	2n, +t(MAC;hChr), +hChr(del)	[14/20]
CHO HSA6p-MAC1 #06	100.0	2n, +t(MAC;hChr), +hChr(del)	[29/30]
CHO HSA21q-MAC2 #01–1	90.0	2n, +t(MAC;hChr), +hChr(del)x2	[22/30]
CHO HSA21q-MAC2 #01–2	85.7	8n, +t(MAC;hChr)x4, +hChr(del)x4, +mar(hChr;MAC)	[2/7]
CHO HSA21q-MAC2 #01–3	100.0	2n, +t(MAC;hChr), +hChr(del)	[7/30]
CHO HSA21q-MAC2 #01–4	94.4	2n, +t(MAC;hChr), +hChr(del)	[5/18]
CHO HSA21q-MAC2 #02–1	46.7	2n, +MAC, +hChr	[12/30]
CHO HSA21q-MAC2 #02–2	0.0	2n, +MAC, +hChr	[4/9]
CHO HSA21q-MAC2 #02–3	66.7	2n, +t(MAC;hChr), +hChr(del)x2	[16/20]

2n: diploid, 4n: tetraploid, 8n: octoploid, +hChr: additional target human chromosome, +MAC: additional mouse artificial chromosome + t(MAC;hChr): hCF-translocated MAC, +hChr(del): deleted target human chromosome.

novel method described herein allows the construction in three steps, consisting of human chromosome labeling in the hiPSCs, direct chromosome transfer, and CRISPR/Cas9-mediated chromosome translocation induction steps (Figure 1B). As a proof of concept, we selected HSA6 and 21, transferred them from hiPSCs into the CHO cell lines containing MAC by the MMCT approach using PTX and Rev, and translocated the isolated chromosomes onto the MAC by CRISPR/Cas9 cleavage while verifying the cloning of hCF-MAC-positive cells by PCR-based screening. Remarkably, this method significantly shortened the time period required for cloning presumably for any hCFs onto the MAC, leading to a more rapid and versatile technology for the subsequent generation of TC animals. This approach is also applicable to chromosome engineering research in general, such as improving the efficiency of aneuploidy cell production by providing an alternative way of human chromosome transfer.

First method for direct transfer of human chromosomes into heterologous cells was reported in the 1980s (37). These protocols demonstrated introducing endogenous *HPRT* gene located chromosome from primary human fibroblast cells (37) or randomly inserted bacterial xanthine-guanine phosphoribosyltransferase gene-carrying chromosomes from tumor cells into mouse cells (38). However, Koi and Oshimura subsequently reported that clones derived from human normal cells transfected with drug resistant genes cannot be used as MMCT donor cells due to reduced proliferative potential caused by finite proliferative capacity and reduced micronucleation efficiency (10). As an alternative, they proposed the use of hybrids of human cells carrying drug-resistant chromosomes and transformed cells, A9, which has been used as the standard protocol to date (11,15). In contrast, the hiPSCs we chose as MMCT donors had infinite proliferative capacity, and chromosome-tagged clones were easily obtained, eliminating the need for hybridization with transformed cells. In addition, when compared with human embryonic stem cells, the use of hiPSCs is minimally invasive, allowing the establishment of cell lines from anyone with less ethical considerations, and when compared with primary somatic cells, it is practical, offering unfathomable prospect of acquiring chromosomes with polymorphisms and disease associations (20). Although our study used a single hiPSC line, it is envisioned that future researchers will use their own established hiPSC lines for chromosome cloning. It is expected that the expansion of patient-derived iPSC resources can provide materials that are convenient not only for acquisition and modification of the regions responsible for diseases, such as hereditary muscle diseases (39) and X-linked diseases involving abnormal satellite copy number of chromosomal regions, but also introduction into mouse models and analysis of human gene expression patterns *in vivo*.

Adapting PTX and Rev which are recently reported as alternatives to colcemid, enabled the formation of micronuclei and harvesting of microcells from hiPSCs, and successful chromosome transfer to CHO cells. As we expected, Rev rescued PTX damage and maintained confluence for 48 hrs. Rev is known to cause chromosomal mis-segregation or polyploidy associated with early mitotic exit by inhibiting a variety of molecules involved in the mitotic checkpoint (28). Although long-term exposure to Rev has been reported to induce cell cycle arrest and apoptosis in cancer cells (40), our results suggest that relatively short-term exposure inhibits PTX-induced spindle checkpoint-induced mitotic cell death. While chromosome-transferred clones were obtained in all independent MMCT trials, HSA21 showed up to 20-fold higher transfer efficiency compared to HSA6 (Table 1). Klinger *et al*. investigating human chromosomal phenotypes by comprehensive karyotyping of tumors derived from human-CHO hybrids reported that additional HSA6 showed significant persistence and non-interference with tumorigenic potential compared to other human chromosomes in the CHO cells, and HSA21 showed a tendency to drop out of the formed tumors (41). This suggests that the phenotypes associated with additional HSA6 and HSA21 in the CHO cells do not correlate with the number of chromosome-transferred clones. While not directly comparable due to the different combinations of recipient cell lines and drug resistance genes, the differences in chromosome size (170 Mb versus 45 Mb) and gene number (≥1900 versus ≥400) between HSA6 and HSA21 are considered as potential factors that may influence MMCT efficiency via microcell size. Chromosome size and gene number are known to positively correlate with micronucleus volume in human cells (42), and there is a concern about the effect on microcell diameter and its filtration process with 8, 5 and 3 μm pore size

of membrane filters. Therefore, it is possible that larger microcells containing HSA6 may be trapped in the filter, resulting in reduced transfer efficiency, although this could be improved by optimizing the minimum pore size. It should be cautioned, however, that this may have the effect of increasing the chance of contamination of microcells with potential multiple chromosomes and should be an issue for future verification.

Although the frequency of genome editing-induced translocations was low, up to 1/15000, we were able to clone them. This indicated that our proposed cell pool seeding and PCR-based screening as stepwise enrichment cloning contributed to high detection sensitivity. Conventional cloning of genome editing-mediated chromosomal translocations has used the concentration process to detect translocated genes associated with the loss of surface markers (43), selection enrichment using drug resistant or fluorescent genes (44,45), and transformation and long-term culture through onco-driver fusion gene formation (22). In contrast, the translocations in this study differ in that they do not result in the loss of surface markers, there is no translocation-specific drug selection, and the effect on cell proliferation is unknown. Thus, this cloning method is a cytogenetic experimental technique that can be used for PCR-detectable and low-frequency mutant cloning as well as translocation detection. However, the translocation efficiency of HSA21q-MAC2 was approximately 10-fold lower than HSA6p-MAC1, although the surveyor assay showed cleavage activity of translocation-induced gRNAs. This suggests the limitation that CRISPR/Cas9 cleavage activity is not a sufficient condition for translocation frequency and the efficiency cannot be predicted and controlled in this study. The formation of translocations requires not only that double-strand breaks occur simultaneously in multiple chromosomes, but also that chromosome fragments come into close proximity in the nucleus and are rejoined by DNA repair. A recent study showed that replication timing is strongly correlated with site-specific translocation efficiency through the formation of replication origins and the subsequent increase in chromatin interactions between different chromosomes (46). Therefore, the simulation of higher order chromatin structure, such as chromosome territories and DNA replisome formation, may contribute to the prediction of translocation hotspots and the design of efficient translocation induction.

We expect that our methodology described herein may be applicable not only to human chromosomes, but also to the cloning and transfer of chromosomes from a wide range of species into heterologous cells via direct MMCT methods and rapid translocation to MACs. Tubulin (a target of PTX) and Mps1 (a target of Rev) are widely conserved in vertebrate (27,47), hence, these proteins when targeted may result in common biological effects across the species. Thus, the use of PTX and Rev, which can induce micronucleus formation while inhibiting mitotic cell death, has the potential to contribute to chromosome transfer in a wide range of vertebrate cells. In addition, chromosomes from multiple species, which is much larger than PAC, BAC, or YAC, can be efficiently loaded into the MACs through genome-editing induced translocations, and chromosomes from heterologous species will be introduced into mice in the future. Taken together, this technology offers a practical solution to eliminate the bottleneck of hCF-MAC construction, and represents a major advance in the field of chromosome or genome engineering that is applicable to a wide range of human chromosome research.

Data availability

All data are incorporated into the article and its online supplementary material.

Supplementary data

Supplementary Data are available at NAR Online.

Acknowledgements

We thank Drs H. Kugoh, M. Hiratsuka, T. Ohira, T. Moriwaki, Y. Yakura, Y. Ohkame, W. Nakagawa and all members of the Chromosome Biomedical Engineering laboratory for critical discussions. Karyotypic analyses were performed at the Tottori Bio Frontier managed by Tottori Prefecture. Graphical abstract was created with BioRender.com.

Author contributions: H.M. wrote the manuscript. H.M., K.Y., S.A. and Y.K. designed the experiment. H.M. and H.K. performed the experiments. N.K., K.Y., N.U. and K.K. provided key materials. K.Y., S.H., S.A and Y.H. edited the manuscript. K.T. and Y.K. supervised the project. All authors critically reviewed the manuscript for intellectual content and approved the final version of the manuscript.

Funding

JST CREST, Japan [JPMJCR18S4 to Y.K.]; Research Support Project for Life Science and Drug discovery (BINDS) from AMED [JP23ama121046 to Y.K.]; Science and Technology Platform Program for Advanced Biological Medicine from AMED [JP23am0401002 to K.T., Y.K.]; AMED [JP23bm1123038 to Y.K., N.U.]; AMED [JP23gm0010010 to Y.K., K.T.]; Joint Research of the Exploratory Research Center on Life and Living Systems (ExCELLS) [ExCELLS program no. 21-101]. Funding for open access charge: JST CREST [JPMJCR18S4].

Conflict of interest statement

None declared.

References

1. Kuroiwa,Y., Yoshida,H., Ohshima,T., Shinohara,T., Ohguma,A., Kazuki,Y., Oshimura,M., Ishida,I. and Tomizuka,K. (2002) The use of chromosome-based vectors for animal transgenesis. *Gene Ther.*, **9**, 708–712.
2. Tomizuka,K., Yoshida,H., Uejima,H., Kugoh,H., Sato,K., Ohguma,A., Hayasaka,M., Hanaoka,K., Oshimura,M. and Ishida,I. (1997) Functional expression and germline transmission of a human chromosome fragment in chimaeric mice. *Nat. Genet.*, **16**, 133–143.
3. Moriwaki,T., Abe,S., Oshimura,M. and Kazuki,Y. (2020) Transchromosomic technology for genomically humanized animals. *Exp. Cell. Res.*, **390**, 111914.
4. Ma,X., Shah,Y., Cheung,C., Guo,G.L., Feigenbaum,L., Krausz,K.W., Idle,J.R. and Gonzalez,F.J. (2007) The pregnane X receptor gene-humanized mouse: a model for investigating drug-drug interactions mediated by cytochromes P450 3A. *Drug Metab. Dispos.*, **35**, 194–200.
5. Yang,Q., Nagano,T., Shah,Y., Cheung,C., Ito,S. and Gonzalez,F.J. (2008) The PPAR alpha-humanized mouse: a model to investigate species differences in liver toxicity mediated by PPAR alpha. *Toxicol. Sci.*, **101**, 132–139.

6. Li,L.P. and Blankenstein,T. (2013) Generation of transgenic mice with megabase-sized human yeast artificial chromosomes by yeast spheroplast-embryonic stem cell fusion. *Nat. Protoc.*, **8**, 1567–1582.
7. Kazuki,K., Takehara,S., Uno,N., Imaoka,N., Abe,S., Takiguchi,M., Hiramatsu,K., Oshimura,M. and Kazuki,Y. (2013) Highly stable maintenance of a mouse artificial chromosome in human cells and mice. *Biochem. Biophys. Res. Commun.*, **442**, 44–50.
8. Kazuki,Y., Gao,F.J., Li,Y.C., Moyer,A.J., Devenney,B., Hiramatsu,K., Miyagawa-Tomita,S., Abe,S., Kazuki,K., Kajitani,N., *et al.* (2020) A non-mosaic transchromosomic mouse model of down syndrome carrying the long arm of human chromosome 21. *eLife*, **9**, e56223. .
9. Kazuki,Y., Kobayashi,K., Hirabayashi,M., Abe,S., Kajitani,N., Kazuki,K., Takehara,S., Takiguchi,M., Satoh,D., Kuze,J., *et al.* (2019) Humanized UGT2 and CYP3A transchromosomic rats for improved prediction of human drug metabolism. *Proc. Nat. Acad. Sci. U.S.A.*, **116**, 3072–3081.
10. Koi,M., Shimizu,M., Morita,H., Yamada,H. and Oshimura,M. (1989) Construction of mouse A9 clones containing a single human-chromosome tagged with neomycin-resistance gene via microcell fusion. *Jpn. J. Cancer Res.*, **80**, 413–418.
11. Nakayama,Y., Adachi,K., Shioda,N., Maeta,S., Nanba,E. and Kugoh,H. (2021) Establishment of FXS-A9 panel with a single human X chromosome from fragile X syndrome-associated individual. *Exp. Cell. Res.*, **398**, 112419.
12. Fournier,R.E.K. and Ruddle,F.H. (1977) Microcell-mediated transfer of murine chromosomes into mouse, chinese-hamster, and human somatic-cells. *Proc. Nat. Acad. Sci. USA*, **74**, 319–323.
13. Kneissig,M., Keuper,K., de Pagter,M.S., van Roosmalen,M.J., Martin,J., Otto,H., Passerini,V., Sparr,A.C., Renkens,I., Kropveld,F., *et al.* (2019) Micronuclei-based model system reveals functional consequences of chromothripsis in human cells. *eLife*, **8**, e50292.
14. Suzuki,T., Kazuki,Y., Oshimura,M. and Hara,T. (2016) Highly efficient transfer of chromosomes to a broad range of target cells using Chinese hamster ovary cells expressing murine leukemia virus-derived envelope proteins. *PLoS One*, **11**, e0157187.
15. Paulis,M., Susani,L., Castelli,A., Suzuki,T., Hara,T., Straniero,L., Duga,S., Strina,D., Mantero,S., Caldana,E., *et al.* (2020) Chromosome transplantation: a possible approach to treat human X-linked disorders. *Mol. Ther. Methods Clin. Dev.*, **17**, 369–377.
16. Yamazaki,K., Matsuo,K., Okada,A., Uno,N., Suzuki,T., Abe,S., Hamamichi,S., Kishima,N., Togai,S., Tomizuka,K., *et al.* (2022) Simultaneous loading of PCR-based multiple fragments on mouse artificial chromosome vectors in DT40 cell for gene delivery. *Sci. Rep.*, **12**, 21790.
17. Kuroiwa,Y., Shinohara,T., Notsu,T., Tomizuka,K., Yoshida,H., Takeda,S., Oshimura,M. and Ishida,I. (1998) Efficient modification of a human chromosome by telomere-directed truncation in high homologous recombination-proficient chicken DT40 cells. *Nucleic Acids Res.*, **26**, 3447–3448.
18. Koi,M., Lamb,P.W., Filatov,L., Feinberg,A.P. and Barrett,J.C. (1997) Construction of chicken x human microcell hybrids for human gene targeting. *Cytogenet. Cell Genet.*, **76**, 72–76.
19. Satofuka,H., Abe,S., Moriwaki,T., Okada,A., Kazuki,K., Tanaka,H., Yamazaki,K., Hichiwa,G., Morimoto,K., Takayama,H., *et al.* (2022) Efficient human-like antibody repertoire and hybridoma production in trans-chromosomic mice carrying megabase-sized human immunoglobulin loci. *Nat. Commun.*, **13**, 1841.
20. Takahashi,K., Tanabe,K., Ohnuki,M., Narita,M., Ichisaka,T., Tomoda,K. and Yamanaka,S. (2007) Induction of pluripotent stem cells from adult human fibroblasts by defined factors. *Cell*, **131**, 861–872.
21. Mout,R., Ray,M., Tonga,G.Y., Lee,Y.W., Tay,T., Sasaki,K. and Rotello,V.M. (2017) Direct cytosolic delivery of CRISPR/Cas9-ribonucleoprotein for efficient gene editing. *ACS Nano*, **11**, 2452–2458.
22. Tamai,M., Fujisawa,S., Nguyen,T.T.T., Komatsu,C., Kagami,K., Kamimoto,K., Omachi,K., Kasai,S., Harama,D., Watanabe,A., *et al.* (2023) Creation of Philadelphia chromosome by CRISPR/Cas9-mediated double cleavages on BCR and ABL1 genes as a model for initial event in leukemogenesis. *Cancer Gene Ther.*, **30**, 38–50.
23. Yumlu,S., Stumm,J., Bashir,S., Dreyer,A.K., Lisowski,P., Danner,E. and Kuhn,R. (2017) Gene editing and clonal isolation of human induced pluripotent stem cells using CRISPR/Cas9. *Methods*, **121**, 29–44.
24. Hussein,S.M., Batada,N.N., Vuoristo,S., Ching,R.W., Autio,R., Narva,E., Ng,S., Sourour,M., Hamalainen,R., Olsson,C., *et al.* (2011) Copy number variation and selection during reprogramming to pluripotency. *Nature*, **471**, 58–U67.
25. Uno,N., Satofuka,H., Miyamoto,H., Honma,K., Suzuki,T., Yamazaki,K., Ito,R., Moriwaki,T., Hamamichi,S., Tomizuka,K., *et al.* (2023) Treatment of CHO cells with Taxol and reversine improves micronucleation and microcell-mediated chromosome transfer efficiency. *Mol.Ther. Nucleic Acids*, **33**, 391–403.
26. Gallaher,B., Berthold,A., Klammt,J., Knupfer,M., Kratzsch,J., Bartsch,M. and Kiess,W. (2000) Expression of apoptosis and cell cycle related genes in proliferating and colcemid arrested cells of divergent lineage. *Cell. Mol. Biol. (Noisy-le-grand)*, **46**, 79–88.
27. Long,B.H. and Fairchild,C.R. (1994) Paclitaxel inhibits progression of mitotic cells to G(1) phase by interference with spindle formation without affecting other microtubule functions during anaphase and telephase. *Cancer Res.*, **54**, 4355–4361.
28. Santaguida,S., Tighe,A., D'Alise,A.M., Taylor,S.S. and Musacchio,A. (2010) Dissecting the role of MPS1 in chromosome biorientation and the spindle checkpoint through the small molecule inhibitor reversine. *J. Cell Biol.*, **190**, 73–87.
29. Uno,N., Hiramatsu,K., Uno,K., Komoto,S., Kazuki,Y. and Oshimura,M. (2017) CRISPR/Cas9-induced transgene insertion and telomere-associated truncation of a single human chromosome for chromosome engineering in CHO and A9 cells. *Sci. Rep.*, **7**, 12739.
30. Liu,Y., Ma,G.W., Gao,Z.H., Li,J., Wang,J., Zhu,X.P., Ma,R.W., Yang,J.W., Zhou,Y.T., Hu,K.S., *et al.* (2022) Global chromosome rearrangement induced by CRISPR-Cas9 reshapes the genome and transcriptome of human cells. *Nucleic Acids Res.*, **50**, 3456–3474.
31. Kazuki,Y., Uno,N., Abe,S., Kajitani,N., Kazuki,K., Yakura,Y., Sawada,C., Takata,S., Sugawara,M., Nagashima,Y., *et al.* (2021) Engineering of human induced pluripotent stem cells via human artificial chromosome vectors for cell therapy and disease modeling. *Mol. Ther. Nucleic Acids*, **23**, 629–639.
32. Takiguchi,M., Kazuki,Y., Hirarnatsu,K., Abe,S., Iida,Y., Takehara,S., Nishida,T., Ohbayashi,T., Wakayama,T. and Oshimura,M. (2014) A novel and stable mouse artificial chromosome vector. *ACS Synth. Biol.*, **3**, 903–914.
33. Tomimatsu,K., Kokura,K., Nishida,T., Yoshimura,Y., Kazuki,Y., Narita,M., Oshimura,M. and Ohbayashi,T. (2017) Multiple expression cassette exchange via TP901-1, R4, and Bxb1 integrase systems on a mouse artificial chromosome. *FEBD Open Biol.*, **7**, 306–317.
34. Yoshimura,Y., Nakamura,K., Endo,T., Kajitani,N., Kazuki,K., Kazuki,Y., Kugoh,H., Oshimura,M. and Ohbayashi,T. (2015) Mouse embryonic stem cells with a multi-integrase mouse artificial chromosome for transchromosomic mouse generation. *Transgenic Res.*, **24**, 717–727.
35. Sawatsubashi,S., Joko,Y., Fukumoto,S., Matsumoto,T. and Sugano,S.S. (2018) Development of versatile non-homologous end joining-based knock-in module for genome editing. *Sci. Rep.*, **8**, 594.
36. Schneider,C.A., Rasband,W.S. and Eliceiri,K.W. (2012) NIH Image to ImageJ: 25 years of image analysis. *Nat. Methods*, **9**, 671–675.
37. McNeill,C.A., Brown,R.L. and Stubblefield,T.E. (1980) Microcell-mediated transfer of single human-chromosomes into recipient mouse cells. *Eur. J. Cell Biol.*, **22**, 587–587.

38. Athwal,R.S., Smarsh,M., Searle,B.M. and Deo,S.S. (1985) Integration of a dominant selectable marker into human-chromosomes and transfer of marked chromosomes to mouse cells by microcell fusion. *Somatic Cell Mol. Genet.*, **11**, 177–187.
39. Mitsuhashi,S., Nakagawa,S., Sasaki-Honda,M., Sakurai,H., Frith,M.C. and Mitsuhashi,H. (2021) Nanopore direct RNA sequencing detects DUX4-activated repeats and isoforms in human muscle cells. *Hum. Mol. Genet.*, **30**, 552–563.
40. Cheng,L., Wang,H., Guo,K.C., Wang,Z.C., Zhang,Z.Y., Shen,C., Chen,L. and Lin,J. (2018) Reversine, a substituted purine, exerts an inhibitive effect on human renal carcinoma cells via induction of cell apoptosis and polyploidy. *Oncotargets Ther.*, **11**, 1025–1035.
41. Klinger,H.P. and Shows,T.B. (1983) Suppression of tumorigenicity in somatic-cell hybrids .2. human-chromosomes implicated as suppressors of tumorigenicity in hybrids with chinese-hamster ovary cells. *J. Natl. Cancer Inst.*, **71**, 559–569.
42. Mammel,A.E., Huang,H.Z., Gunn,A.L., Choo,E. and Hatch,E.M. (2022) Chromosome length and gene density contribute to micronuclear membrane stability. *Life Sci. Allian.*, **5**, e202101210.
43. Kitano,Y., Nishimura,S., Kato,T.M., Ueda,A., Takigawa,K., Umekage,M., Nomura,M., Kawakami,A., Ogawa,H., Xu,H.G., *et al.* (2022) Generation of hypoimmunogenic induced pluripotent stem cells by CRISPR-Cas9 system and detailed evaluation for clinical application. *Mol. Ther. Methods Clin. Dev.*, **26**, 15–25.
44. Torres-Ruiz,R., Martinez-Lage,M., Martin,M.C., Garcia,A., Bueno,C., Castano,J., Ramirez,J.C., Menendez,P., Cigudosa,J.C. and Rodriguez-Perales,S. (2017) Efficient recreation of t(11;22) EWSR1-FLI1(+) in human stem cells using CRISPR/Cas9. *Stem Cell Rep.*, **8**, 1408–1420.
45. van Ijzendoorn,D.G.P., Salvatori,D.C.F., Cao,X., van den Hil,F., Briaire-de Bruijn,I.H., de Jong,D., Mei,H.L., Mummery,C.L., Szuhai,K., Bovee,J., *et al.* (2020) Vascular Tumor Recapitulated in endothelial cells from hiPSCs engineered to express the SERPINE1-FOSB translocation. *Cell Rep. Med.*, **1**, 100153.
46. Peycheva,M., Neumann,T., Malzl,D., Nazarova,M., Schoeberl,U.E. and Pavri,R. (2022) DNA replication timing directly regulates the frequency of oncogenic chromosomal translocations. *Science*, **377**, eabj5502.
47. Yamagishi,Y., Yang,C.H., Tanno,Y. and Watanabe,Y. (2012) MPS1/Mph1 phosphorylates the kinetochore protein KNL1/Spc7 to recruit SAC components. *Nat. Cell Biol.*, **14**, 746–752.

Received: August 29, 2023. **Revised:** November 26, 2023. **Editorial Decision:** December 9, 2023. **Accepted:** January 3, 2024